Kent Academic Repository
Full text document (pdf)

Splitting of multiple hydrogen molecules by bioinspired diniobium metal complexes: a DFT study

ARTICLE

Splitting of multiple hydrogen molecules by bioinspired diniobium metal complexes: a DFT study

Felipe Fantuzzi,[abc] Marco Antonio Chaer Nascimento,*[a] Bojana Ginovska,[b] R. Morris Bullock[b] and Simone Raugei*[b]

Splitting of molecular hydrogen (H_2) into bridging and terminal hydrides is a common step in transition metal chemistry. Herein, we propose a novel organometallic platform for cleavage of multiple H_2 molecules, which combines metal centers capable of stabilizing multiple oxidation states, and ligands bearing positioned pendant basic groups. Using quantum chemical modeling, we show that low-valent, early transition metal diniobium(II) complexes with diphosphine ligands featuring pendant amines can favorably uptake up to 8 hydrogen atoms, and that the energetics are favored by the formation of intramolecular dihydrogen bonds. This result suggests new possible strategies for the development of hydrogen scavenger molecules that are able to perform reversible splitting of multiple H_2 molecules.

Introduction

The search for molecules and materials that are able to bind and split molecular hydrogen (H_2) has been the focus of intense research for decades. Different classes of systems have shown activity towards such chemical transformation, including carbon-based materials,[1] frustrated Lewis pairs (FLPs),[2] metal hydrides,[3] complex hydrides,[4] metal-organic frameworks (MOFs)[5] and metal cluster complexes.[6] It is known that mono- and polynuclear metal complexes and clusters are able to store relatively large amounts of hydrogen in the form of hydride ligands.[7] However, even while recognizing the remarkable progress made in recent years, current hydrogen storage materials still present large heats of H_2 absorption and low volumetric H_2 loads. The optimum heat of H_2 adsorption for effective storage and release of the H_2 gas at practical temperatures (-40 to +80 °C) and pressures (1 to 700 bar) has been estimated to be in the range of 5-12 kcal (mol H_2)$^{-1}$.[8] These values have been adopted as optimal target for H_2 storage materials by the United States Department of Energy (US DOE).[9] To the best of our knowledge, no materials have met the H_2 binding enthalpies or capacity metrics set by the US DOE.[5a]

Herein, we provide design principles for dinuclear coordination compounds with improved capabilities for splitting multiple H_2 molecules. We propose to use transition metals capable of stabilizing multiple oxidation states, such as Nb, and positioned pendant basic groups to stabilize multiple metal hydrides *via* dihydrogen bonds, *i.e.*, intramolecular hydride-proton interactions.[10] Indeed, the

computational investigation reported here shows that low-valent, early diniobium(II) compounds could bind and cleave up to four H_2 molecules. Our findings provide inspiration for the design of novel hydrogen sponges based on the formation of strong dihydrogen bonds.[10]

Niobium is known for its very rich redox chemistry, with oxidation states ranging from +5 to –3.[11] The abundance of Nb in some parts of the Earth,[12] especially Brazil and Canada, has motivated our interest to search for potential applications for this metal. Previous work exploring the catalytic activity of Nb have shown that this metal is particularly effective towards hydrogen splitting[7a,13] and shows rich polyhydride chemistry.[14-16] Specifically, niobium has the tendency to form dinuclear or polynuclear complexes,[17] which offer the opportunity to bind multiple hydrides. In this work, we focus on the experimentally-realized, low-valent triply bonded Nb_2^{4+} core.[18] The first examples of low-valent Nb_2 species are the anionic face-sharing bioctahedral complexes of the type $[Nb_2X_6(THT)_3]^{2-}$, X = Cl or Br and THT = tetrahydrothiophene (Fig. 1a, left), $[Nb_2Cl_5(THT)(py)_3]^-$, py = pyridine, and $[Nb_2Cl_7(PR_3)]^-$, R = Me, Et. These complexes feature rather long metal–metal bond distances (ca. 2.6-2.7 Å).[19] By using chelating anionic ligands, Cotton *et al*. were able to isolate neutral, diamagnetic Nb_2L_4 compounds featuring a paddle-wheel coordination (Fig 1a, center) and remarkably short metal–metal bond distances (ca. 2.2-2.3 Å).[20] These species can form adducts with $NaEt_3BH$ and LiCl,[20b,21] with only small changes in the Nb–Nb bond lengths.[22] A series of compounds having Nb_2^{q+} core, *q* = 4, 6, and 8, were obtained by stabilization with calix[4]arene ligands.[23] Some of them present activity towards the stepwise reduction of dinitrogen to nitride. Dinitrogen cleavage and its subsequent conversion into imide species by a $[Nb_2(\mu-H)_4(RO_3)_2]^{2-}$ complex[14a] was also observed, which is formally obtained by the splitting of two dihydrogen molecules into a Nb_2^{4+} core and whose reactivity shows counterion dependence.[14b] This compound was the focus of a recent and extensive computational study by Luo and others.[24] A similar neutral $Nb_2(\mu-H)_4(ArO)_4$ compound (Fig 1a, right)

[a.] *Instituto de Química, Universidade Federal do Rio de Janeiro, Av. Athos da Silveira Ramos 149, 21941.909, Rio de Janeiro, Brazil. E-mail: chaer01@gmail.com*
[b.] *Center for Molecular Electrocatalysis, Pacific Northwest National Laboratory, Richland, WA 99352, USA. E-mail: simone.raugei@pnnl.gov*
[c.] *Institute for Inorganic Chemistry, Julius-Maximilians-Universität Würzburg, Am Hubland, 97074, Würzburg, Germany.*
Electronic Supplementary Information (ESI) available: electronic and thermochemical properties of selected Nb_2^{4+} species; cartesian coordinates. See DOI: 10.1039/x0xx00000x

ARTICLE
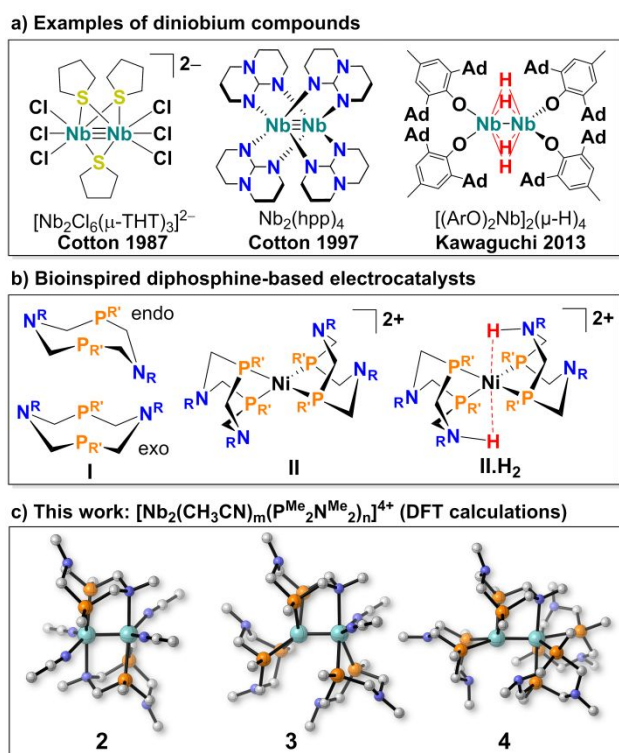
Figure 1 a) Left: the anionic $[Nb_2Cl_6(THT)_3]^{2-}$ species;[19a] middle: the paddle-wheel $Nb_2(hpp)_4$ complex,[20a] hpp = 1,3,4,6,7,8-hexahydropyrimido[1,2-a]pyrimidinate; Right: the tetrahydride $Nb_2(\mu\text{-}H)_4(ArO)_4$ compound.[15] b) Left: the 1,5-R-3,7-R'-1,5-diaza-3,7-diphosphacyclooctane ligand **I**, with conformations that lead to endo (top) and exo (bottom) coordination after metal complexation; middle: a Ni(II) bioinspired diphosphine-based electrocatalyst **II**,[30] in which both ligands are in the endo configuration. Right: endo-endo isomer of **II.H$_2$** featuring two N–H bonds and a Ni(0) center.[30] c) starting $[Nb_2(CH_3CN)_m(P^{Me}_2N^{Me}_2)_n]^{4+}$ (**2**, n = 2, m = 4; **3**, n = 3, m = 2 ; **4**, n = 4, m = 0) optimized structures used for the study of hydrogen uptake and splitting. Niobium: green; phosphorus: orange; nitrogen: blue; carbon: gray.

is able to reduce CO *via* hydrogenation and deoxygenation, leading to a methylidene-bridged compound.[15] Low-valent Nb compounds have also shown reactivity towards C–C[25] and C–N multiple bonds, including intermolecular cycloaddition of alkynes and nitriles,[26] reductive nitrile coupling,[27] unorthodox mixed $\eta^2(3e)$-nitrile/$\eta^2(3e)$-alkyne coordination,[28] and metal–metal cleavage by nitriles to form mononuclear Nb(V) imido species.[29]

Here we report an extensive exploration of the free energy landscape of multiple H_2 activation and splitting by Nb_2^{4+} with 1,5-R-3,7-R'-1,5-diaza-3,7-diphospha-cyclooctane ($P^R_2N^{R'}_2$) ligands (**I**, see Fig. 1b) in acetonitrile (CH_3CN) solution. $P^R_2N^{R'}_2$ ligands have been successfully used in the development of Ni (**II** and **II.H$_2$**, see Fig. 1b)[30] and Fe[31] electrocatalysts for hydrogen oxidation and production. The incorporation of amine groups next to the metal center is a common functionality of bioinspired synthetic catalysts mimicking the diaza bridge of the catalytic cofactor of [FeFe]-hydrogenases.[32] In the case

of bimetallic polyhydride compounds, the presence of pendant amines could enhance the number of active H_2 molecules through the formation of distinct hydride-proton interaction pairs. Such intramolecular interactions could be formed between (i) the pendant amine proton and a bridging hydride, (ii) the pendant amine proton and a terminal hydride, or (iii) in a three-center proton-dihydride fashion. While similar examples of (i) and (ii) are commonly found in the literature,[33] only the intermolecular version of (iii) has been observed up to now, as in the case of the NH···H$_2$Re interaction reported by Wessel and co-workers.[34]

The coordination of the $(P^R_2N^{R'}_2)$ ligand to the metal through the P atoms leads to the formation of two six-membered rings, which adopt either chair or boat conformations. Protonation of a pendant amine of a ring in a chair conformation favors chair conformers stabilized by intramolecular NH···N hydrogen bonding (exo protonation),[30a] which are detrimental for the formation of the desired dihydrogen bonds. On the other hand, protonation of six-membered rings in a boat conformation leads to N–H moieties that are oriented toward the metal center. Only these pendant amines are properly positioned to produce dihydrogen bonding with bridging and terminal hydrides (endo protonation). In order to design compounds that could activate multiple H_2 molecules using such intramolecular interaction, the six-membered rings containing participating pendant amines are retained in boat conformations, while the spectator ones are in chair conformations (see **II.H$_2$** of Fig. 1 for an illustration of such structures). In *bona fide* catalysts, the preference for boat over chair conformation can be tuned by changing the nature of the substituents on both phosphorus and nitrogen.[35] For computational simplicity, herein we focus on methyl substituted ligands ($P^{Me}_2N^{Me}_2$).

Computational Details

We performed geometry optimizations and Hessian calculations at the B3LYP[36] -D3(BJ)[37]/def2-SVP[38] level of theory. For the optimized structures, we performed additional single-point calculations using B3LYP-D3(BJ) and M06[39]-D3 with the def2-TZVPP basis set. Solvent effects were considered using the integral equation formalism polarizable continuum model (IEFPCM, solvent: acetonitrile, ε = 35.688).[40] Previous computational studies have been reported where B3LYP was satisfactorily used to describe the geometries and electronic structures of Nb_2^{4+} core compounds.[41] Indeed, the computation of experimentally known diniobium systems performed by us at the B3LYP-D3(BJ)/def2-SVP level of theory also indicated a very good agreement between experiments and theory (see Table S15). Additionally, previous work from us and others showed that the computational setup adopted herein is appropriate to study hydrogen uptake and splitting by a variety of transition metal complexes.[24,30,31,42] In this regard, we point out the recent benchmarking study of H_2 uptake developed by Veccham and Head-Gordon,[42f] who recommended the combination of empirical dispersion corrections and def2-TZVPP basis set for improving the performance of B3LYP. In all our calculations the 28 core electrons of Nb were described using the quasi-relativistic effective core potential def2-ECP.[43] The Gibbs free energies at 298.15 K of all species were calculated by combining the electronic energies from the single point

ARTICLE
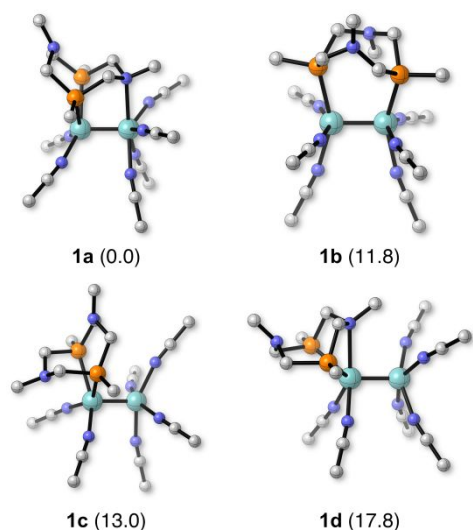
Figure 2 Lowest free energy isomers of $[Nb_2(CH_3CN)_6(P^{Me}_2N^{Me}_2)_n]^{4+}$ (n = 1) calculated in acetonitrile at the B3LYP-D3(BJ)/def2-TZVPP//B3LYP-D3(BJ)/def2-SVP level of theory. Relative free energies in kcal mol^{-1} are given in parentheses.

calculations with the thermochemical corrections based on harmonic vibration frequencies obtained at the same level of theory used for geometry optimization. In addition, we included a free energy concentration correction of $\Delta G^{0\rightarrow*}$ = RTln(24.46) = 1.89 kcal mol^{-1} for all species in order to account for the change in standard states in going from gas phase (1 atm) to the condensed phase (1 M), and to properly describe associative/dissociative steps.[44] For acetonitrile, a standard state concentration of 19.15 mol L^{-1} was used, leading to a total correction of $\Delta G^{0\rightarrow*}$ = 3.64 kcal mol^{-1}. All systems were described at their singlet states using spin-restricted wave functions. Additional spin-unrestricted calculations considering initially antiferromagnetic coupled metal centers converged to the spin-restricted solutions, while calculations for higher multiplicities (triplet and quintet) converged to high-energy states.

The formation of mono-, di-, tri- and tetra-substituted $Nb_2L_n^{4+}$ species in CH_3CN solution, as well as their propensity to bind and cleave H_2, was evaluated by calculating the free energy of the reaction shown in eq. 1 for several number of ligands (n), coordination solvent molecules (m) and bound H_2 molecules (k). We will refer to this energy as the free energy of complex formation, ΔG_b.

$$[Nb_2(CH_3CN)_8]^{4+} + nL + kH_2 \rightarrow [Nb_2(CH_3CN)_m(L)_n(H_2)_k]^{4+} + (8-m)\, CH_3CN \qquad (1)$$
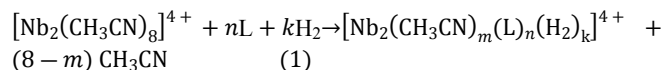
Corrections for basis set superposition error (BSSE) were not taken into account as we find that a good compromise between accuracy and computational cost is obtained by using counterpoise-uncorrected interaction energies calculated with def2-TZVPP.[42f] The quantities obtained using either B3LYP-D3(BJ) or M06-D3 functionals are in reasonable agreement. Therefore, unless otherwise stated, all energy values are the ones obtained at the B3LYP-D3(BJ) level. The calculations were carried out using Gaussian 16, Revision B.01[45] after pre-optimization in NWChem 6.8.[46] Images of 3D structures and plots
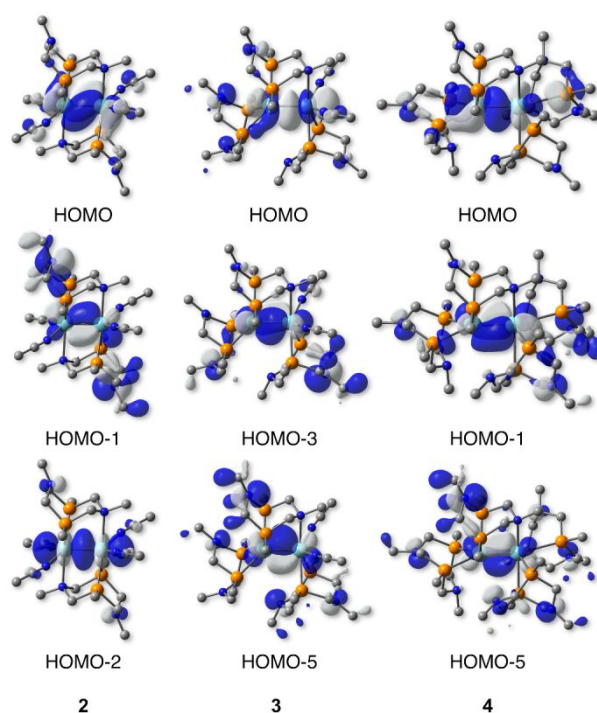
Figure 3 Frontier Kohn-Sham MOs of $[Nb_2(CH_3CN)_m(P^{Me}_2N^{Me}_2)_n]^{4+}$ (**2**, n = 2, m = 4; **3**, n = 3, m = 2 ; **4**, n = 4, m = 0) calculated at the B3LYP-D3(BJ)/def2-TZVPP//B3LYP-D3(BJ)/def2-SVP level of theory.

of frontier Kohn-Sham molecular orbitals (MOs) were obtained using CYLview[47] and Gaussview, respectively.

Results and Discussion

Molecular Design of the Starting Structures
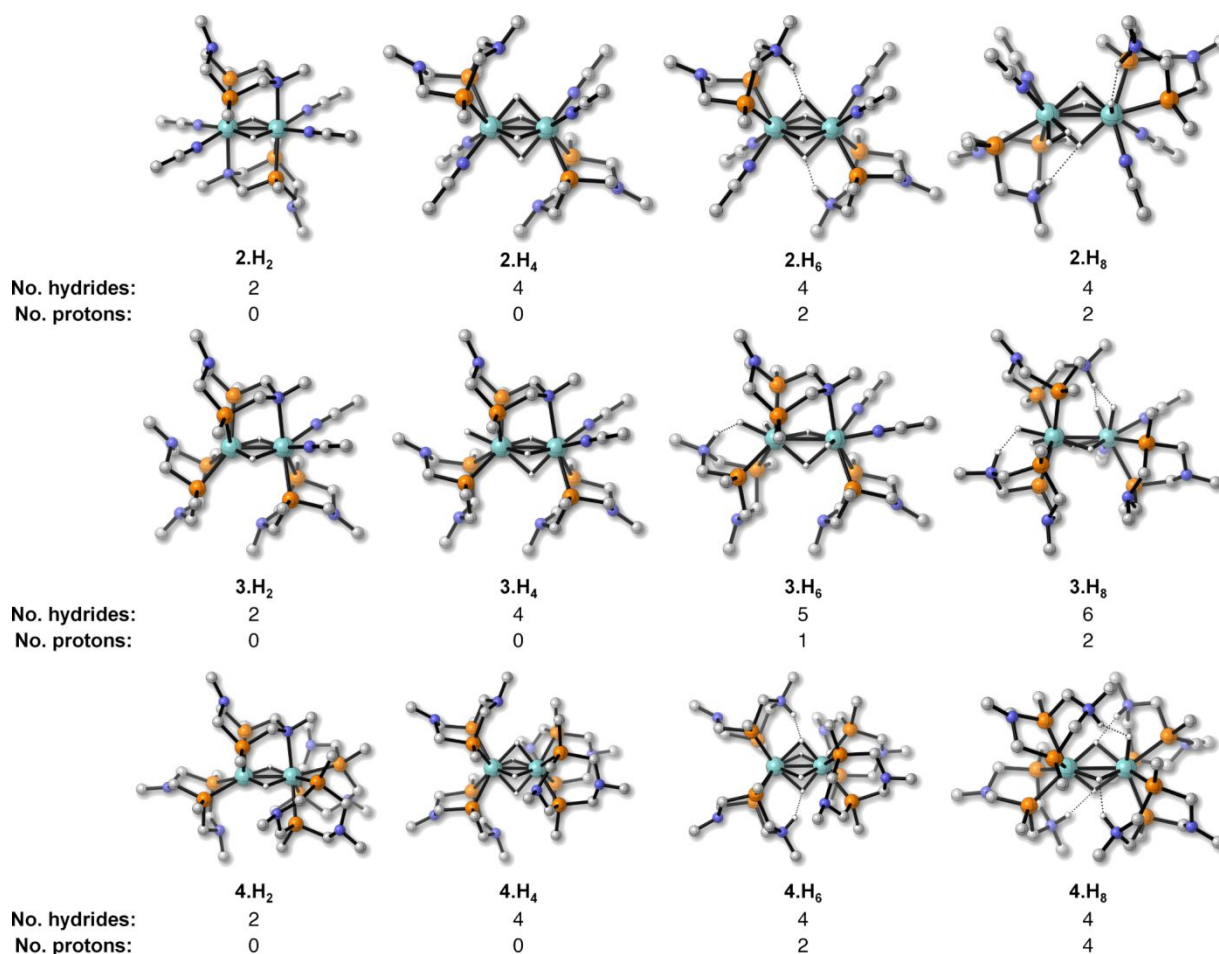
Figure 4 Optimized structures of the most stable [Nb$_2$(CH$_3$CN)$_m$(P$^{Me}_2$N$^{Me}_2$)$_n$(H$_2$)$_k$]$^{4+}$ isomers of **2.(H$_2$)$_k$** (*n* = 2, *m* = 4), **3.(H$_2$)$_k$** (*n* = 3, *m* = 2) and **4.(H$_2$)$_k$** (*n* = 4, *m* = 0), with *k* = 1-4, at the B3LYP-D3(BJ)/def2-SVP level of theory. The number of hydrides and protons of each structure after multiple H$_2$ splitting is also shown. **2.H$_8$** features a dihydrogen ligand coordinated to one of the niobium atoms (see text for details).

We started our computational investigation by building model diniobium systems using the paddle-wheel complex Nb$_2$(hpp)$_4$ (see Fig. 1c) as a structural template. Each of the Nb–N bonding interaction in Nb$_2$(hpp)$_4$ was replaced by coordinating CH$_3$CN molecules, leading to [Nb$_2$(CH$_3$CN)$_8$]$^{4+}$. Additional calculations indicated that this is indeed the most stable diniobium species in neat acetonitrile (see section S1 for details), and therefore was used as reference state in the ΔG_b calculations. We found that the [Nb$_2$(CH$_3$CN)$_8$]$^{4+}$ complex can give rise to a very rich speciation chemistry, as it can coordinate two (*n* = 2), three (*n* = 3) and four (*n* = 4) diphosphine ligands L in several distinct manners. We then performed a thorough exploration of the harmonic free energy landscape of the [Nb$_2$(CH$_3$CN)$_m$(P$^{Me}_2$N$^{Me}_2$)$_n$]$^{4+}$ compounds, and identified the most abundant species present in acetonitrile solution by using eq. 1 and considering *k* = 0. Starting from [Nb$_2$(CH$_3$CN)$_8$]$^{4+}$, we replaced two of the CH$_3$CN molecules by one diphosphine ligand P$^{Me}_2$N$^{Me}_2$, leading to [Nb$_2$(CH$_3$CN)$_6$(P$^{Me}_2$N$^{Me}_2$)]$^{4+}$ (**1a-d**, Fig. 2). We found four distinct isomers of **1**, the most stable (**1a**) having P$^{Me}_2$N$^{Me}_2$ as a bridging ligand in a tridentate 1κ^2-P,2κ^1-N binuclear coordination type, where κ describes the denticity of the ligand. In this case, the

phosphorus atoms of each ligand are coordinated to the same Nb center, while the pendant amine coordinates to the other Nb center. By progressively replacing the other coordinating solvent molecules, we obtained the complexes **2** [Nb$_2$(CH$_3$CN)$_4$(P$^{Me}_2$N$^{Me}_2$)$_2$]$^{4+}$, **3** [Nb$_2$(CH$_3$CN)$_2$(P$^{Me}_2$N$^{Me}_2$)$_3$]$^{4+}$ and **4** [Nb$_2$(P$^{Me}_2$N$^{Me}_2$)$_4$]$^{4+}$ (Fig. 1). In fact, the sequential displacement of two coordinating CH$_3$CN molecules by one P$^{Me}_2$N$^{Me}_2$ ligand produced the complexes with most negative ΔG_b values (see Tables S3, S5 and S12), revealing that **2-4** are the best starting structures among the ones obtained herein for investigating multiple hydrogen splitting. In these systems, at least one of the diphosphine ligands binds to the Nb$_2^{4+}$ core in the same coordination mode as the one in **1a**. Additional isomers of **2-4** that were obtained by our calculations are also depicted in sections S4-S12.

Fig. 3 shows the structures and the relevant frontier Kohn-Sham MOs of complexes **2-4**. In **2**, both P$^{Me}_2$N$^{Me}_2$ ligands are coordinated to the metal dimer in the tridentate 1κ^2-P,2κ^1-N binuclear coordination type also featured in **1a**. Examples of similar coordination of the pendant base have been observed for Mn[48] and Cr[49] mononuclear metal complexes, resulting in stable κ^3 systems, while for Ni and Co this feature has not been observed. Moreover, κ^3

ARTICLE
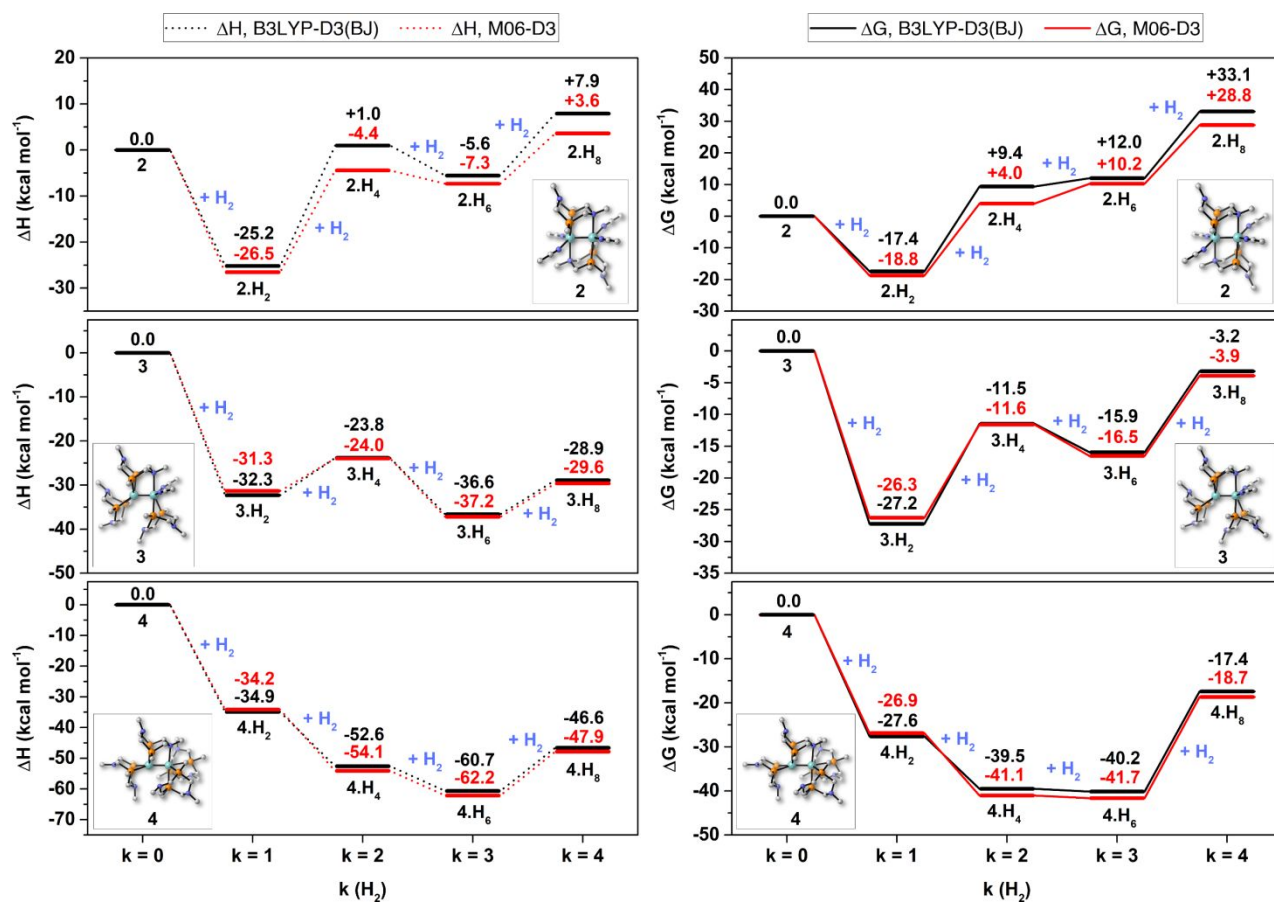
Figure 5 Thermochemical profile of multiple H_2 splitting on $[Nb_2(CH_3CN)_m(P^{Me}_2N^{Me}_2)_n]^{4+}$ (top: **2**, $n = 2$, $m = 4$; middle: **3**, $n = 3$, $m = 2$; bottom: **4**, $n = 4$, $m = 0$), following the most stable $[Nb_2(CH_3CN)_m(P^{Me}_2N^{Me}_2)_n(H_2)_k]^{4+}$ isomers for each stoichiometry. Panels on the left show the ΔH values for B3LYP-D3(BJ)/def2-TZVPP+PCM and M06-D3/def2-TZVPP+PCM (298.15 K) with respect to the number of H_2 molecules (structures were optimized at B3LYP-D3(BJ)/def2-SVP). Panels on the right show the respective ΔG values obtained at the same levels of calculation.

binding of an azadithiolate ligand was also found in a [FeFe]-hydrogenase model complex, as reported by Rauchfuss and co-workers.[50]

The acetonitrile ligands in compound **2** are coordinated to each Nb center in equatorial positions. In principle, the binding of H_2 could be achieved by an initial dissociation of either the pendant amine or one of the coordinating acetonitrile molecules. While examples of isomers featuring H_2 binding after dissociation of acetonitrile groups were found (e.g. **2.2**), our attempts to optimize complexes featuring H_2 after pendant amine dissociation failed. In this case, they converged to a system featuring an NH···HNb interaction whose free energy is 47.5 kcal mol^{-1} above **2.H$_2$** (see structure **(2.H$_2$)b** in section S5). This result suggests that most likely the first H_2 addition in **2** is preceded by an initial acetonitrile dissociation as we discuss later.

The very short Nb–Nb bond distance (2.37 Å) in structure **2** is in the range of the Nb$_2$L$_4$ complexes featuring metal–metal triple bonds. The triple bond character of Nb–Nb is also supported by the frontier Kohn-Sham MOs, for which the HOMO and HOMO-1 are heavily centered on the π space of the Nb$_2$ moiety, while HOMO-2 is a σ-type orbital lying on the intermetallic vector.

The lowest free energy isomer of $[Nb_2(CH_3CN)_2(P^{Me}_2N^{Me}_2)_3]^{4+}$ (**3**) presents a mixed phosphine-to-metal coordination. One ligand binds to the two Nb centers in a tridentate $1\kappa^2$-P,$2\kappa^1$-N binuclear coordination type as in **2**, whereas the other two ligands are coordinating the metals in a bidentate κ^2-P mononuclear fashion, similarly to the one in **1c**. The additional acetonitrile ligands bind to the same Nb atom. This leads to an asymmetric coordination environment for each metal center, with the presence of tetra- and penta-coordinated metal centers. The Nb–Nb bond distance (2.34 Å) is just slightly shortened in comparison to **2** and, as in the previous case, the shape of the frontier Kohn-Sham MOs also suggests that the metals are triply bonded.

The most stable isomer with four $P^{Me}_2N^{Me}_2$ ligands, $[Nb_2(P^{Me}_2N^{Me}_2)_4]^{4+}$ (**4**), also features one diphosphine in the tridentate $1\kappa^2$-P,$2\kappa^1$-N bridging mode, while the remaining isomers have bidentate κ^2-P ligands. Isomers in which the four diphosphines behave as κ^2-P ligands or in which two of the diphosphines coordinate the bimetallic moiety in the $1\kappa^2$-P, $2\kappa^1$-N bridging mode were not found. The Nb–Nb bond is slightly elongated to 2.41 Å, most likely due to steric repulsion from the
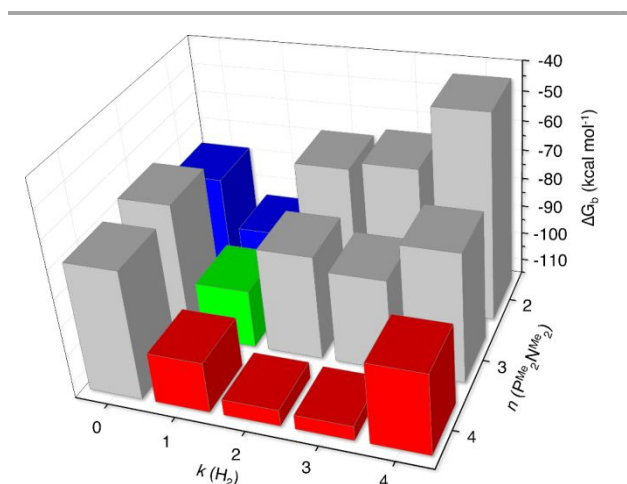
Figure 6 Speciation free energy landscape of $[Nb_2(CH_3CN)_m(P^{Me}_2N^{Me}_2)_n(H_2)_k]^{4+}$. Gray bars indicate high energy species, while the colored bars show intermediates involved in the lowest free energy pathway from **2** (n = 2, m = 4, k = 0) to **4.H$_8$** (n = 4, m = 0, k = 4). Blue: species with n = 2; green: species with n = 3; red: species with n = 4. Energies were obtained at the B3LYP-D3(BJ)/def2-TZVPP+PCM level following eq. 1.

phosphine groups. Nevertheless, it still is in the range of a triple bond, which is also supported by the frontier Kohn-Sham MOs.

Multiple hydrogen splitting by 2-4

All of the $[Nb_2(CH_3CN)_m(P^{Me}_2N^{Me}_2)_n]^{4+}$ species discussed above are able to uptake and break the H–H bond of four H_2 molecules. Many different isomers differing in the location of the hydrogen atoms are possible. Upon uptake of H_2, association and dissociation of $P^{Me}_2N^{Me}_2$ ligands are possible, which can give rise to complex speciation equilibria in acetonitrile solution. We found that the Nb_2 core can accommodate up to four hydrides in bridging positions, or up to six hydrides considering both bridging and terminal positions. The pendant amines can host up to four protons. Based on previous studies on mononuclear doubly protonated $[Ni(P_2^RN_2^{R'})_2]^0$ complexes, we are expecting equilibria between various isomers, which involves intra- and inter-molecular protonation/deprotonation steps.[30a,51] In the present study, we limited our focus on the identification of the possible lowest-free energy isomers. Possible speciation pathways will be discussed based on simple thermodynamic arguments.

We start by discussing the various hydride coordination motifs and dihydrogen bonding featured in the $[Nb_2(CH_3CN)_m(P^{Me}_2N^{Me}_2)_n(H_2)_k]^{4+}$ complexes, as shown in Fig. 4. We will do this by focusing on the complexes with n = 2, 3, and 4 after the uptake of three and four H_2 molecules (k = 3 and 4, respectively), as they provide an illustration of the rich variety of possible bonding motifs in this class of complexes. This discussion is accompanied by the DFT calculated enthalpies and free energies at 298.15 K of each hydrogenated species with respect to their respective isolated diniobium complexes and H_2 molecules in acetonitrile solution, as depicted in Fig. 5.

The most stable isomer of **2** upon uptake of three H_2 molecules, **2.H$_6$**, is the tetrahydride species with two protonated amines. All of the hydrides are bridging the two metal centers, reducing the Nb–Nb bond order and leading consequently to an increase in the metal–metal bond distance to 2.60 Å. Additionally, formation of the tetrahydride motif causes the loss of the pendant amine N coordination. The two N–H bonds in **2.H$_6$** point towards the bridging hydrides, and the proton–hydride distances of d(H···H) ~ 1.60 Å suggest presence of two dihydrogen bonds. This value is just moderately larger than the remarkably short H···H distance of 1.49 Å observed for an [FeFe]-hydrogenase model, as revealed by neutron diffraction,[52] and by far shorter than the sum of the van der Waals radii of the H atoms (2.4 Å). The ΔH of **2.H$_6$** is more negative than the one of **2** by 5.6 kcal mol^{-1}, which indicates that the polyhydride formation assisted by dihydrogen bonding is able to compensate for the loss of two Nb–N bonds. However, due to entropic reasons, the ΔG of this process is positive by 12.0 kcal mol^{-1}, indicating that addition of the third H_2 molecule to **2** is not favorable. Addition of a fourth H_2 molecule to **2.H$_6$** leads to **2.H$_8$**, located 33.1 kcal mol^{-1} above **2**. The system contains three bridging hydrides, one terminal hydride, two protonated amines and a dihydrogen moiety. The Nb–Nb bond length is 2.77 Å, in the range of a single bond.[19c] No other bonded structure was found with such stoichiometry.

Complex **3** can accommodate six H atoms (three H_2 molecules, **3.H$_6$**) while retaining the tridentate $1\kappa^2$-P,$2\kappa^1$-N coordination. Complex **3.H$_6$** features two bridging hydrides, two terminal hydrides (one on each metal center), and one protonated amine. An NH···HNb distance of 1.53 Å is observed, indicating the presence of dihydrogen bonding, which might contribute to the ΔH lowering of 12.8 kcal mol^{-1} from **3.H$_4$**. On the other hand, the κ^3 coordination motif in **3.H$_8$** is broken, and the fourth H_2 binds across the ancillary Nb–N bond. As a consequence, a slightly distorted three-center dihydride-proton interaction is observed, with NH···H$_2$Nb bond distances of 1.62 and 1.64 Å. Activation and splitting of three and four H_2 molecules are favorable by ΔG = –15.9 and –3.2 kcal mol^{-1}, respectively. The uphill character of the fourth H_2 addition in **3** could be attributed mainly to the breaking of the Nb–N bond, and to the fact that the stabilizing contribution of the subsequent dihydrogen bonding is not able to compensate for the unfavorable energetics of this bond dissociation.

Complex **4.H$_6$** has C_2 symmetry and can host up to four bridging hydrides and two protonated amines, which interact via strong two-center dihydrogen bonds with the hydrides (d(H···H) = 1.76 Å). The ΔH of this complex is –60.7 kcal mol^{-1}, and its formation from **4** is favorable by ΔG = –40.2 kcal mol^{-1}. The addition of a fourth H_2 molecule causes the migration of one bridging hydride to a terminal position and the protonation of all four pendant amines. As a consequence, **4.H$_8$** has four dihydrogen bonds: three of them involving bridging hydride and an N–H proton, and the remaining one coming from a terminal hydride/(amine) proton interaction. The transformation of **4.H$_6$** to **4.H$_8$** is uphill by 22.8 kcal mol^{-1}, following the increase in the enthalpy of 14.1 kcal mol^{-1}, probably due to the breakage of the $[Nb_2(\mu-H_4)]$ bonding motif. However, the formation of **4.H$_8$** from **4** is still quite favorable (ΔG = –17.4 kcal mol^{-1}), suggesting the viability of obtaining such hydrogen-rich system.

Lowest energy pathway from ΔG_b calculations
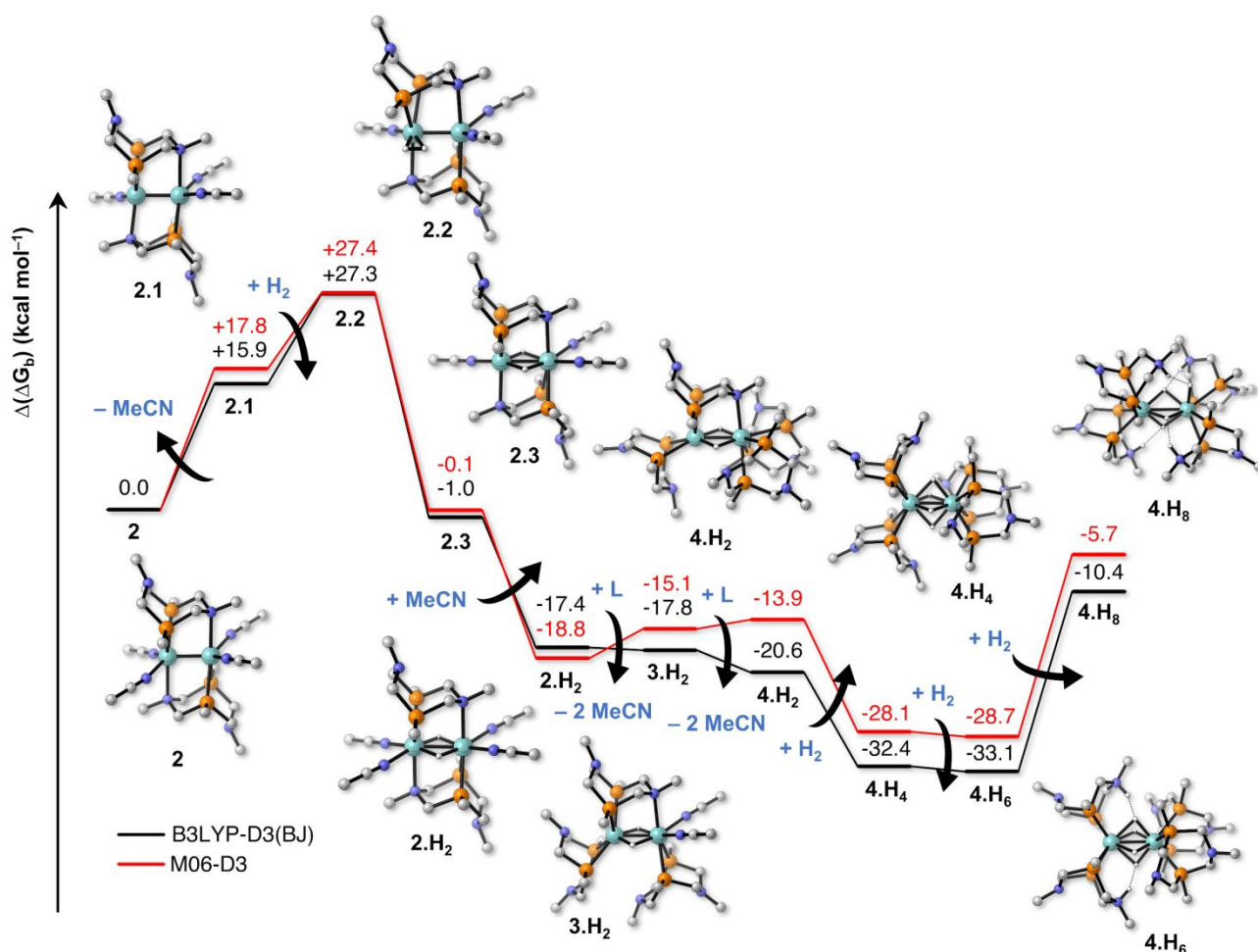
Figure 7 Free energy profile of the lowest-energy pathway of $[Nb_2(CH_3CN)_m(P^{Me}_2N^{Me}_2)_n(H_2)_k]^{4+}$ connecting **2** (n = 2, m = 4, k = 0) and **4.H₈** (n = 4, m = 0, k = 4). Black curve: B3LYP-D3(BJ)/def2-TZVPP+PCM; red curve: M06-D3/def2-TZVPP+PCM (structures were optimized at B3LYP-D3(BJ)/def2-SVP). L = the diphosphine ligand $P^{Me}_2N^{Me}_2$.

From the free energies of complex formation (ΔG_b), it is possible to build a 3D bar diagram (Fig. 6) that shows the speciation of the diniobium systems in acetonitrile solution with respect to the number and type of coordinating molecules. In this plot, each bar represents the ΔG_b of a particular species calculated according to eq. 1. The higher the bar, the less probable is the formation of the intermediate. The number of H_2 molecules uptaken (k = 0-4) and the number of $P^{Me}_2N^{Me}_2$ ligands (n = 2-4) are indicated on the x and y axis, respectively. The resulting free energy map can be used to predict possible low-energy reaction pathways for the uptake of H_2 molecules by this class of Nb complexes.[30c] While this approach does not address the kinetic feasibility of each individual chemical step, it provides a lower bound of the activation barrier for any possible transformation connecting two species in free energy map.

The most stable species in acetonitrile solution for k = 0 is **2**. Starting from this species, we analyze the pathway that connects the lowest-energy intermediates for multiple H_2 activation. The replacement of two MeCN in **2** by a diphosphine ligand, leading to **3**, is followed by an increase of $\Delta(\Delta G_b)$ = +9.5 kcal mol⁻¹. However, the attachment of the first H_2 leading to **2.H₂** is exergic, with $\Delta(\Delta G_b)$ = −

17.4 kcal mol⁻¹. Therefore, our results suggest that the first step should be H_2 addition to **2**. A similar consideration indicates that the next step is the nearly isoergic conversion of **2.H₂** into **3.H₂**, with $\Delta(\Delta G_b)$ = −0.4 kcal mol⁻¹. Addition of a fourth diphosphine ligand leads to **4.H₂**, $\Delta(\Delta G_b)$ = −2.8 kcal mol⁻¹, which then favorably binds a second H_2 ($\Delta(\Delta G_b)$ = −11.9 kcal mol⁻¹) yielding **4.H₄**. The latter can uptake a third H_2 in a nearly isoergic reaction ($\Delta(\Delta G_b)$ = −0.6 kcal mol⁻¹), producing **4.H₆**. Among all structures, this is the one with the most negative free energy of complex formation. Its conversion to **4.H₈** after a fourth H_2 uptake is uphill by $\Delta(\Delta G_b)$ = +22.7 kcal mol⁻¹. Although this step is unfavorable, the formation of **4.H₈** is still exergic with respect to **2**, with $\Delta(\Delta G_b)$ = −10.4 kcal mol⁻¹.

The lowest free energy pathway for multiple hydrogen addition, together with the energetics involved in the transformation of **2** to **2.H₂** following H_2 addition, are depicted altogether in Fig. 7. As can be seen, the highest free energy value is related to the formation of the dihydrogen complex **2.2** after acetonitrile dissociation (+27.3 kcal mol⁻¹ above **2**). Addition of the subsequent H_2 molecules takes advantage of the

very favorable conversion of **2** to **2.H₂**, which helps overcome any further unfavorable step for multiple hydrogen splitting.

Conclusions

In summary, we have illustrated a novel strategy for activating and splitting multiple H₂ molecules, which makes use of complexes capable of stabilizing multiple oxidation states, such as Nb, and pendant bases in the second coordination sphere. Quantum chemical calculations on $[Nb_2(CH_3CN)_m(P^{Me}_2N^{Me}_2)_n]^{4+}$ show that this type of molecular platform could allow storing up to 8 electrons and 8 protons (four H₂ molecules). The highest hydrogen-to-metal ratio (4:1) of the systems studied herein is achieved by either accumulating four hydrides on the Nb_2^{4+} moiety and four protons on the pendant amines, or six hydrides on the Nb_2^{4+} moiety and two protons on the pendant amines. In the case of $[Nb_2(CH_3CN)_2(P^{Me}_2N^{Me}_2)_3]^{4+}$ and $[Nb_2(P^{Me}_2N^{Me}_2)_4]^{4+}$ uptake of up to four H₂ molecules is thermodynamically favorable. Formation of stable hydrides is clearly undesired for hydrogen storage as it hampers its release. Ideally, one would like to have nearly isoergic accumulation of protons and electrons. As demonstrated by the vast body of our work,[30d] the diaza-diphosphine ligands adopted here can be easily functionalized by changing the substituents on the P and N atoms, facilitating the tuning of the hydricity and acidity of the protonated metal centers and the acid/base properties of the pendant amines. Consequently, this allows for a fine tuning of the relative energetic of possible proton/electron accumulation intermediates. Future research should be devoted to design ligand sets that nearly flatten the free energy landscape of Fig. 6.[30c]

Conflicts of interest

There are no conflicts to declare.

Acknowledgements

Notes and references

1   (a) T. Yildirim and S. Ciraci, *Phys. Rev. Lett.*, 2005, **94**, 175501; (b) T. Yildirim, J. Íñiguez and S. Ciraci, *Phys. Rev. B*, 2005, **72**, 153403; (c) T. D. Della and C. H. Suresh, *Phys. Chem. Chem. Phys.*, 2017, **19**, 5830–5838; (d) L.-J. Ma, J. Wang, M. Han, J. Jia, H.-S. Wu and X. Zhang, *Int. J. Hydrogen Energy*, 2019, **44**, 18145–18152; (e) O. Faye, T. Hussain, A. Karton and J. Szpunar, *Nanotechnology*, 2019, **30**, 075404; (f) M. Mohan, V. K. Sharma, E. A. Kumar and V. Gayathri, *Energy Storage*, 2019, **1**, e35; (g) L.-L. Ma, Y. Rong and T. Han, *Int. J. Hydrogen Energy*, 2020, **45**, 15302–15316.

2   (a) G. C. Welch, R. R. San Juan, J. D. Masuda and D. W. Stephan, *Science*, 2006, **314**, 1124–6; (b) D. W. Stephan and G. Erker, *Angew. Chem. Int. Ed. Engl.*, 2010, **49**, 46–76; (c) Z. Dong, Z. Li, X. Liu, C. Yan, N. Wei, M. Kira and T. Müller, *Chem. - An Asian J.*, 2017, **12**, 1204–1207.

3   (a) A. Züttel, *Mater. Today*, 2003, **6**, 24–33; (b) N. V. Belkova, L. M. Epstein, O. A. Filippov and E. S. Shubina, *Chem. Rev.*, 2016, **116**, 8545–8587; (c) E. Mamontov, A. I. Kolesnikov, S. Sampath and J. L. Yarger, *Sci. Rep.*, 2017, **7**, 16244.

4   (a) M. B. Ley, L. H. Jepsen, Y.-S. Lee, Y. W. Cho, J. M. Bellosta von Colbe, M. Dornheim, M. Rokni, J. O. Jensen, M. Sloth, Y. Filinchuk, J. E. Jørgensen, F. Besenbacher and T. R. Jensen, *Mater. Today*, 2014, **17**, 122–128; (b) T. He, H. Cao and P. Chen, *Adv. Mater.*, 2019, **31**, 1902757; (c) C. Milanese, T. R. Jensen, B. C. Hauback, C. Pistidda, M. Dornheim, H. Yang, L. Lombardo, A. Zuettel, Y. Filinchuk, P. Ngene, P. E. de Jongh, C. E. Buckley, E. M. Dematteis and M. Baricco, *Int. J. Hydrogen Energy*, 2019, **44**, 7860–7874.

5   (a) M. T. Kapelewski, T. Runčevski, J. D. Tarver, H. Z. H. Jiang, K. E. Hurst, P. A. Parilla, A. Ayala, T. Gennett, S. A. FitzGerald, C. M. Brown and J. R. Long, *Chem. Mater.*, 2018, **30**, 8179–8189; (b) A. Ahmed, S. Seth, J. Purewal, A. G. Wong-Foy, M. Veenstra, A. J. Matzger and D. J. Siegel, *Nat. Commun.*, 2019, **10**, 1568; (c) V. R. Bakuru, M. E. DMello and S. B. Kalidindi, *ChemPhysChem*, 2019, **20**, 1177–1215.

6   (a) T. G. M. M. Kappen, J. J. Bour, P. P. J. Schlebos, A. M. Roelofsen, J. G. M. Van der Linden, J. J. Steggerda, M. A. Aubart, D. A. Krogstad, M. F. J. Schoondergang and L. H. Pignolet, *Inorg. Chem.*, 1993, **32**, 1074–1075; (b) P. J. Dyson and J. S. McIndoe, *Angew. Chem. Int. Ed.*, 2005, **44**, 5772–5774; (c) J.-H. Meng and S.-G. He, *J. Phys. Chem. Lett.*, 2014, **5**, 3890–3894.

7   (a) R. R. Schrock, *J. Organomet. Chem.*, 1976, **121**, 373–379; (b) R. D. Adams, M. P. Pompeo and W. Wu, *Inorg. Chem.*, 1991, **30**, 2425–2432; (c) R. Shimogawa, T. Takao and H. Suzuki, *J. Organomet. Chem.*, 2016, **818**, 168–178; (d) L. Omann, C. D. F. Königs, H. F. T. Klare and M. Oestreich, *Acc. Chem. Res.*, 2017, **50**, 1258–1269; (e) J. I. Fostvedt, T. D. Lohrey, R. G. Bergman and J. Arnold, *Chem. Commun.*, 2019, **55**, 13263–13266.

8   J. Yang, A. Sudik, C. Wolverton and D. J. Siegel, *Chem. Soc. Rev.*, 2010, **39**, 656–675.

9   (a) Progress Report for the DOE Hydrogen and Fuel Cells Program (2018). www.nrel.gov/publications (accessed May 25, 2020); (b) L. E. Klebanoff, K. C. Ott, L. J. Simpson, K. O'Malley and N. T. Stetson, *Metall. Mater. Trans. E*, 2014, **1**, 81–117.

10   (a) R. H. Crabtree, P. E. M. Siegbahn, O. Eisenstein, A. L. Rheingold and T. F. Koetzle, *Acc. Chem. Res.*, 1996, **29**, 348–354; (b) R. Custelcean and J. E. Jackson, *Chem. Rev.*, 2001, **101**, 1963–1980.

11   (a) L. G. Hubert-Pfalzgraf, in *Encyclopedia of Inorganic and Bioinorganic Chemistry*, John Wiley & Sons, Ltd, Chichester, UK, 2011; (b) M. A. Tarselli, *Nat. Chem.*, 2015, **7**, 180–180.

12   (a) D. A. Wyman, J. A. Ayer and J. R. Devaney, *Earth Planet. Sci. Lett.*, 2000, **179**, 21–30; (b) P. F. de O. Cordeiro, J. A. Brod, M.

Palmieri, C. G. de Oliveira, E. S. R. Barbosa, R. V. Santos, J. C. Gaspar and L. C. Assis, *Ore Geol. Rev.*, 2011, **41**, 112–121; (c) D. A. R. Mackay and G. J. Simandl, *Miner. Depos.*, 2014, **49**, 1025–1047; (d) A. R. Alves and A. dos R. Coutinho, *Mater. Res.*, 2015, **18**, 106–112; (e) R. H. Mitchell, *Ore Geol. Rev.*, 2015, **64**, 626–641.

13 (a) G. W. Parshall and F. N. Tebbe, *J. Am. Chem. Soc.*, 1971, **93**, 3793–3795; (b) K. W. Chiu, R. A. Jones, G. Wilkinson, A. M. R. Galas and M. B. Hursthouse, *J. Chem. Soc., Dalt. Trans.*, 1981, 1892–1897; (c) S. Niaz, T. Manzoor, N. Islam and A. H. Pandith, *Int. J. Quantum Chem.*, 2014, **114**, 449–457; (d) G. Liu, S. Besedin, A. Irodova, H. Liu, G. Gao, M. Eremets, X. Wang and Y. Ma, *Phys. Rev. B*, 2017, **95**, 104110.

14 (a) F. Akagi, T. Matsuo and H. Kawaguchi, *Angew. Chem. Int. Ed.*, 2007, **46**, 8778–8781; (b) S. Suzuki, Y. Ishida, S. Kameo, S. Sakaki and H. Kawaguchi, *Angew. Chem. Int. Ed.*, 2020, **59**, 13444–13450.

15 T. Kurogi, Y. Ishida, T. Hatanaka and H. Kawaguchi, *Dalt. Trans.*, 2013, **42**, 7510–7513.

16 (a) A. Antinolo, B. Chaudret, G. Commenges, M. Fajardo, F. Jalon, R. H. Morris, A. Otero and C. T. Schweltzer, *J. Chem. Soc., Chem. Commun.*, 1988, 1210–1212; (b) A. Antiñolo, F. Carrillo-Hermosilla, J. Fernández-Baeza, S. García-Yuste, A. Otero, J. Sánchez-Prada and E. Villaseñor, *Eur. J. Inorg. Chem.*, 2000, **2000**, 1437–1443.

17 C. A. Murillo, *Inorg. Chim. Acta*, 2017, **468**, 3–15.

18 F. A. Cotton, C. A. Murillo and R. A. Walton, *Multiple Bonds Between Metal Atoms*; Eds.; Springer-Verlag: New York, 2005; pp 29–33.

19 (a) F. A. Cotton, M. P. Diebold and W. J. Roth, *J. Am. Chem. Soc.*, 1987, **109**, 5506–5514; (b) F. A. Cotton and M. Shang, *Inorg. Chem.*, 1993, **32**, 969–976; (c) F. A. Cotton and M. Shang, *Inorg. Chim. Acta*, 1994, **227**, 191–196.

20 (a) F. A. Cotton, J. H. Matonic and C. A. Murillo, *J. Am. Chem. Soc.*, 1997, **119**, 7889–7890; (b) F. A. Cotton, J. H. Matonic and C. A. Murillo, *J. Am. Chem. Soc.*, 1998, **120**, 6047–6052.

21 M. Tayebani, K. Feghali, S. Gambarotta, G. P. A. Yap and L. K. Thompson, *Angew. Chem. Int. Ed.*, 1999, **38**, 3659–3661.

22 M. Tayebani, K. Feghali, S. Gambarotta and G. P. A. Yap, *Inorg. Chem.*, 2001, **40**, 1399–1401.

23 (a) A. Zanotti-Gerosa, E. Solari, L. Giannini, C. Floriani, A. Chiesi-Villa and C. Rizzoli, *J. Am. Chem. Soc.*, 1998, **120**, 437–438; (b) A. Caselli, E. Solari, R. Scopelliti and C. Floriani, *J. Am. Chem. Soc.*, 1999, **121**, 8296–8305; (c) A. Caselli, E. Solari, R. Scopelliti and C. Floriani, *J. Am. Chem. Soc.*, 2000, **122**, 538–539; (d) A. Caselli, E. Solari, R. Scopelliti, C. Floriani, N. Re, C. Rizzoli and A. Chiesi-Villa, *J. Am. Chem. Soc.*, 2000, **122**, 3652–3670.

24 J. Yang, G. Luo, Y. Yu, J. Qu, Z. Hou and Y. Luo, *Inorg. Chem.*, 2020, **59**, 4626–4633.

25 (a) F. A. Cotton and M. Shang, *Inorg. Chem.*, 1990, **29**, 508–514; (b) F. A. Cotton and M. Shang, *J. Am. Chem. Soc.*, 1990, **112**, 1584–1590; (c) F. A. Cotton and M. Shang, *Inorg. Chem.*, 1990, **29**, 2614–2618; (d) F. A. Cotton and M. Shang, *Inorg. Chem.*, 1990, **29**, 2619–2622; (e) F. A. Cotton and X. Feng, *Inorg. Chem.*, 1990, **29**, 3697–3701; (f) F. A. Cotton and M. Shang, *Organometallics*, 1990, **9**, 2131–2137.

26 Y. Satoh and Y. Obora, *J. Org. Chem.*, 2013, **78**, 7771–7776.

27 B. M. Reinhard, A. Lagutschenkov, J. Lemaire, P. Maitre, P. Boissel and G. Niedner-Schatteburg, *J. Phys. Chem. A*, 2004, **108**, 3350–3355.

28 M. Etienne, C. Carfagna, P. Lorente, R. Mathieu and D. de Montauzon, *Organometallics*, 1999, **18**, 3075–3086.

29 F. A. Cotton, G. Wilkinson, C. A. Murillo and M. Bochmann, *Advanced Inorganic Chemistry*, John Wiley & Sons, New York, 6th edn., 1999.

30 (a) M. O'Hagan, W. J. Shaw, S. Raugei, S. Chen, J. Y. Yang, U. J. Kilgore, D. L. Dubois and R. M. Bullock, *J. Am. Chem. Soc.*, 2011, **133**, 14301–14312; (b) S. Raugei, S. Chen, M.-H. Ho, B. Ginovska-Pangovska, R. J. Rousseau, M. Dupuis, D. L. DuBois and R. M. Bullock, *Chem. - A Eur. J.*, 2012, **18**, 6493–6506; (c) S. Raugei, D. L. DuBois, R. Rousseau, S. Chen, M.-H. Ho, R. M. Bullock and M. Dupuis, *Acc. Chem. Res.*, 2015, **48**, 248–255; (d) S. Raugei, M. L. Helm, S. Hammes-Schiffer, A. M. Appel, M. O'Hagan, E. S. Wiedner and R. M. Bullock, *Inorg. Chem.*, 2016, **55**, 445–460.

31 (a) T. Liu, D. L. DuBois and R. M. Bullock, *Nat. Chem.*, 2013, **5**, 228–233; (b) T. Liu, Q. Liao, M. O'Hagan, E. B. Hulley, D. L. DuBois and R. M. Bullock, *Organometallics*, 2015, **34**, 2747–2764.

32 (a) H.-J. Fan and M. B. Hall, *J. Am. Chem. Soc.*, 2001, **123**, 3828–3829; (b) J. C. Fontecilla-Camps, A. Volbeda, C. Cavazza and Y. Nicolet, *Chem. Rev.*, 2007, **107**, 4273–4303; (c) C. Sommer, C. P. Richers, W. Lubitz, T. B. Rauchfuss and E. J. Reijerse, *Angew. Chem. Int. Ed.*, 2018, **57**, 5429–5432; (d) F. Arrigoni, L. Bertini, M. Bruschi, C. Greco, L. De Gioia and G. Zampella, *Chem. - A Eur. J.*, 2019, **25**, 1227–1241.

33 R. M. Bullock and G. M. Chambers, *Philos. Trans. R. Soc. A Math. Phys. Eng. Sci.*, 2017, **375**, 20170002.

34 J. Wessel, J. C. Lee, E. Peris, G. P. A. Yap, J. B. Fortin, J. S. Ricci, G. Sini, A. Albinati, T. F. Koetzle, O. Eisenstein, A. L. Rheingold and R. H. Crabtree, *Angew. Chem. Int. Ed. English*, 1995, **34**, 2507–2509.

35 (a) M. Rakowski DuBois and D. L. DuBois, *Chem. Soc. Rev.*, 2009, **38**, 62–72; (b) A. J. P. Cardenas, B. Ginovska, N. Kumar, J. Hou, S. Raugei, M. L. Helm, A. M. Appel, R. M. Bullock and M. O'Hagan, *Angew. Chem. Int. Ed.*, 2016, **55**, 13509–13513.

36 (a) S. H. Vosko, L. Wilk and M. Nusair, *Can. J. Phys.*, 1980, **58**, 1200–1211; (b) C. Lee, W. Yang and R. G. Parr, *Phys. Rev. B*, 1988, **37**, 785–789; (c) A. D. Becke, *J. Chem. Phys.*, 1993, **98**, 5648–5652; (d) P. J. Stephens, F. J. Devlin, C. F. Chabalowski and M. J. Frisch, *J. Phys. Chem.*, 1994, **98**, 11623–11627.

37 (a) S. Grimme, J. Antony, S. Ehrlich and H. Krieg, *J. Chem. Phys.*, 2010, **132**, 154104; (b) S. Grimme, S. Ehrlich and L. Goerigk, *J. Comput. Chem.*, 2011, **32**, 1456–1465.

38 F. Weigend and R. Ahlrichs, *Phys. Chem. Chem. Phys.*, 2005, **7**, 3297.

39 Y. Zhao and D. G. Truhlar, *Theor. Chem. Acc.*, 2008, **120**, 215–241.

40 (a) V. Barone, M. Cossi and J. Tomasi, *J. Chem. Phys.*, 1997, **107**, 3210–3221; (b) M. Cossi, G. Scalmani, N. Rega and V. Barone, *J. Chem. Phys.*, 2002, **117**, 43–54; (c) J. Tomasi, B. Mennucci and R. Cammi, *Chem. Rev.*, 2005, **105**, 2999–3094.

41 (a) F. A. Cotton and X. Feng, *J. Am. Chem. Soc.*, 1997, **119**, 7514–7520; (b) M. N. Sokolov, A. L. Gushchin, S. V. Tkachev, D. Y. Naumov, P. Nuñez, P. Gili, J. G. Platas and V. P. Fedin, *Inorg. Chim. Acta*, 2005, **358**, 2371–2383; (c) R. Hernandez-Molina, P. Gili, M. N. Sokolov and V. S. Safont, *Inorg. Chim. Acta*, 2011, **376**, 10–17; (d) L. N. Mazalov, A. D. Fedorenko, G. K. Parygina, A. L. Gushchin, M. N. Sokolov and S. A. Dalmatova, *J. Struct. Chem.*, 2017, **58**, 1625–1632.

42 (a) S. Chen, S. Raugei, R. Rousseau, M. Dupuis and R. M. Bullock, *J. Phys. Chem. A*, 2010, **114**, 12716–12724; (b) G. Zeng and S. Sakaki, *Inorg. Chem.*, 2013, **52**, 2844–2853; (c) D. Senthilnathan, P. Giunta, V. Vetere, A. Kachmar, P. Maldivi and A. A. Franco, *RSC Adv.*, 2014, **4**, 5177; (d) W. Wang, J. Wang, L. Huang and H. Wei, *Catal. Sci. Technol.*, 2015, **5**, 2157–2166; (e) A. M. Lunsford, J. H. Blank, S. Moncho, S. C. Haas, S. Muhammad, E. N. Brothers, M. Y. Darensbourg and A. A. Bengali, *Inorg. Chem.*, 2016, **55**, 964–973; (f) S. P. Veccham and M. Head-Gordon, *J. Chem. Theory Comput.*, 2020, **16**, 4963–4982.

43 D. Andrae, U. Häußermann, M. Dolg, H. Stoll and H. Preuß, *Theor. Chim. Acta*, 1990, **77**, 123–141.

44 (a) C. P. Kelly, C. J. Cramer and D. G. Truhlar, *J. Chem. Theory Comput.*, 2005, **1**, 1133–1152; (b) M. Sparta, C. Riplinger and

F. Neese, *J. Chem. Theory Comput.*, 2014, **10**, 1099–1108; (c) A. Hermann, F. Fantuzzi, M. Arrowsmith, T. Zorn, I. Krummenacher, B. Ritschel, K. Radacki, B. Engels and H. Braunschweig, *Angew. Chemie Int. Ed.*, 2020, **59**, 15717–15725.

45 M. J. Frisch, G. W. Trucks, H. B. Schlegel, G. E. Scuseria, M. A. Robb, J. R. Cheeseman, G. Scalmani, V. Barone, B. Mennucci, G. A. Petersson, H. Nakatsuji, M. Caricato, X. Li, H. P. Hratchian, A. F. Izmaylov, J. Bloino, G. Zheng, J. L. Sonnenberg, M. Hada, M. Ehara, K. Toyota, R. Fukuda, J. Hasegawa, M. Ishida, T. Nakajima, Y. Honda, O. Kitao, H. Nakai, T. Vreven, J. A. Montgomery Jr., J. E. Peralta, F. Ogliaro, M. Bearpark, J. J. Heyd, E. Brothers, K. N. Kudin, V. N. Staroverov, R. Kobayashi, J. Normand, K. Raghavachari, A. Rendell, J. C. Burant, S. S. Iyengar, J. Tomasi, M. Cossi, N. Rega, J. M. Millam, M. Klene, J. E. Knox, J. B. Cross, V. Bakken, C. Adamo, J. Jaramillo, R. Gomperts, R. E. Stratmann, O. Yazyev, A. J. Austin, R. Cammi, C. Pomelli, J. W. Ochterski, R. L. Martin, K. Morokuma, V. G. Zakrzewski, G. A. Voth, P. Salvador, J. J. Dannenberg, S. Dapprich, A. D. Daniels, Ö. Farkas, J. B. Foresman, J. V Ortiz, J. Cioslowski and D. J. Fox, Gaussian 16, Revision B.01, Gaussian, Inc., Wallingford CT, 2016.

46 M. Valiev, E. J. Bylaska, N. Govind, K. Kowalski, T. P. Straatsma, H. J. J. Van Dam, D. Wang, J. Nieplocha, E. Apra, T. L. Windus and W. A. de Jong, *Comput. Phys. Commun.*, 2010, **181**, 1477–1489.

47 C. Y. Legault, CYLview, version 1.0.561b, Université de Sherbrooke, Sherbrooke, QC, Canada, 2009; http://www.cylview.org.

48 E. B. Hulley, M. L. Helm and R. M. Bullock, *Chem. Sci.*, 2014, **5**, 4729–4741.

49 M. T. Mock, S. Chen, R. Rousseau, M. J. O'Hagan, W. G. Dougherty, W. S. Kassel, D. L. DuBois and R. M. Bullock, *Chem. Commun.*, 2011, **47**, 12212.

50 M. T. Olsen, T. B. Rauchfuss and S. R. Wilson, *J. Am. Chem. Soc.*, 2010, **132**, 17733–17740.

51 M. O'Hagan, M.-H. Ho, J. Y. Yang, A. M. Appel, M. R. DuBois, S. Raugei, W. J. Shaw, D. L. DuBois and R. M. Bullock, *J. Am. Chem. Soc.*, 2012, **134**, 19409–19424.

52 T. Liu, X. Wang, C. Hoffmann, D. L. DuBois and R. M. Bullock, *Angew. Chem. Int. Ed.*, 2014, **53**, 5300–5304.
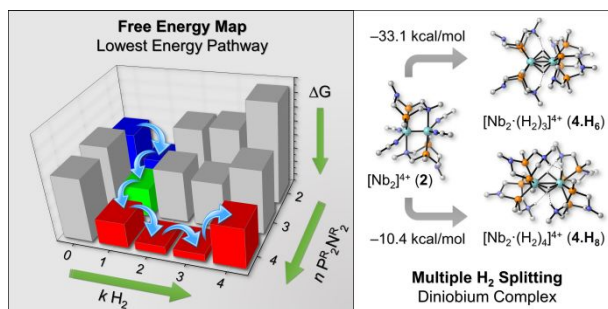
A novel organometallic platform for activation and splitting of multiple H_2 molecules is investigated by quantum chemical calculations.